PROCEEDINGS OF SCIENCE

Inclusive Jets in PHP

Philipp Roloff[*†]
CERN
E-mail: philipp.roloff@cern.ch

Differential inclusive-jet cross sections have been measured in photoproduction for boson virtualities $Q^2 < 1$ GeV^2 with the ZEUS detector at HERA using an integrated luminosity of 300 pb^{-1}. Jets were identified in the laboratory frame using the k_T, anti-k_T or SIScone jet algorithms. Cross sections are presented as functions of the jet pseudorapidity, $\eta^{\rm jet}$, and the jet transverse energy, $E_T^{\rm jet}$. Next-to-leading-order QCD calculations give a good description of the measurements, except for jets with low $E_T^{\rm jet}$ and high $\eta^{\rm jet}$. The cross sections have the potential to improve the determination of the PDFs in future QCD fits. Values of $\alpha_s(M_Z)$ have been extracted from the measurements based on different jet algorithms. In addition, the energy-scale dependence of the strong coupling was determined.

The European Physical Society Conference on High Energy Physics
18-24 July 2013
Stockholm, Sweden

*Speaker.
†On behalf of the ZEUS collaboration.

PoS(EPS-HEP 2013)452

1. Introduction

The measurement of jet photoproduction (PHP) at HERA provides a high-statistics test of perturbative QCD (pQCD) in a process with a single hard scale, $E_T^{\rm jet}$. Jet cross sections allow precise determinations of the strong coupling constant, α_s, and its energy dependence.

At leading order, so-called direct and resolved processes contribute to jet photoproduction. In direct processes, the photon interacts directly with a parton in the proton. On the other hand, the photon acts as a source of partons for the resolved contributions. Hence inclusive-jet cross sections are directly sensitive to the proton and photon PDFs.

The k_T cluster algorithm [1] in the longitudinally invariant inclusive mode [2] results in small theoretical uncertainties and hadronisation corrections in electron-proton collisions. It yields infrared- and collinear-safe cross sections at any order of QCD. More recently, new infrared- and collinear-safe algorithms like anti-k_T [3] or SIScone [4] were developed. Jet photoproduction at HERA represents a well-understood hadron-induced reaction to test and compare the performances of these different jet clustering algorithms.

NLO QCD predictions [5] are compared to the measured inclusive-jet cross sections. The renormalisation and factorisation scales were set to $\mu_R = \mu_F = E_T^{\rm jet}$ and the number of flavours was chosen to be five. Unless explicitly stated otherwise, the ZEUS-S [6] parametrisations were used for the proton PDFs and the GRV-HO [7] sets were chosen for the photon PDFs. Hadronisation corrections were obtained using the `Pythia` [8] and `Herwig` [9] Monte Carlo (MC) programs. For comparisons, samples of `Pythia` including multi-parton interactions [10], `Pythia-MI`, were used to estimate the contribution from non-perturbative effects not related to hadronisation. For all three jet algorithms introduced above, missing terms beyond NLO represent the dominant uncertainty of the predictions.

2. Differential inclusive-jet cross sections

Single- and double-differential inclusive-jet cross sections have been measured in the reaction $ep \to e + {\rm jet} + {\rm X}$ for $142 < W_{\gamma p} < 293$ GeV, where $W_{\gamma p}$ is the γp centre-of-mass energy, and $Q^2 < 1$ GeV^2 with the ZEUS detector at HERA using an integrated luminosity of 300 pb^{-1}. The cross sections include every jet with $E_T^{\rm jet} > 17$ GeV and $-1 < \eta^{\rm jet} < 2.5$ [11].

Single-differential cross sections based on the k_T algorithm as functions of $E_T^{\rm jet}$ and $\eta^{\rm jet}$ are shown in Fig. 1. The uncertainty on the jet energy scale of $\pm 1\%$ typically leads to a $\mp 5\%$ uncertainty on the measured cross sections which is fully correlated between measurements in different bins. At high $E_T^{\rm jet}$ this uncertainty increases to $\mp 10\%$. The measurements are well described by NLO QCD except for $\eta^{\rm jet} > 2$. The disagreement in the forward region disappears if the kinematic region of the measurement is restricted to $E_T^{\rm jet} > 21$ GeV.

Alternative NLO QCD predictions based on the HERAPDF1.5 [12] and MSTW08 [13] proton PDFs instead of ZEUS-S are also shown in Fig. 1. The predictions based on HERAPDF1.5 are lower than those based on ZEUS-S in most of the investigated phase-space region. Especially at large $E_T^{\rm jet}$, the usage of MSTW08 instead of ZEUS-S in the NLO QCD calculations leads to higher predictions. The high-precision measurements of inclusive-jet photoproduction have the potential to constrain the proton PDFs in future QCD fits.

PoS(EPS-HEP 2013)452

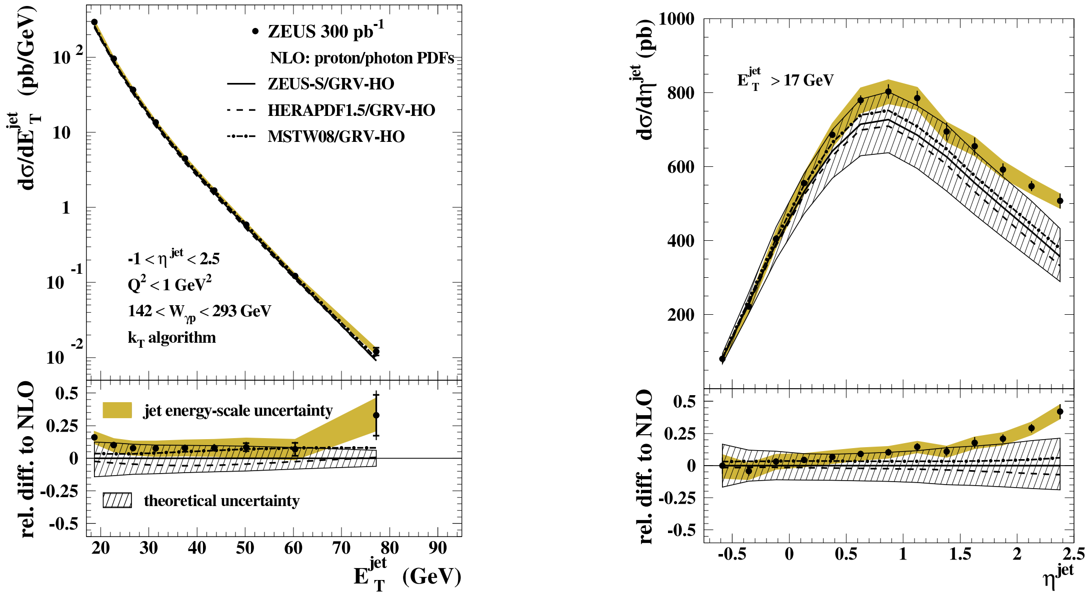

Figure 1: Single-differential cross sections $d\sigma/dE_T^{\rm jet}$ (left) and $d\sigma/d\eta^{\rm jet}$ (right) based on the k_T algorithm. The data are compared to NLO QCD predictions based on different proton PDFs.

In addition, inclusive-jet cross sections based on the k_T algorithm were determined as functions of $E_T^{\rm jet}$ in different regions of $\eta^{\rm jet}$. As observed for the single differential cross sections, the data are well described by NLO QCD except at $E_T^{\rm jet} < 21$ GeV for $\eta^{\rm jet} > 2$.

3. Impact of multi-parton interactions

The effect of multi-parton interactions is not included in the NLO QCD calculations described in Sec. 1. Instead, correction factors were obtained using `Pythia-MI` including multi-parton interactions with a minimum transverse momentum of the secondary scatter, $p_{T,\rm min}^{\rm sec}$, of 1, 1.5 and 2 GeV. Single-differential cross sections based on the k_T algorithm as functions of $E_T^{\rm jet}$ and $\eta^{\rm jet}$ are compared to NLO QCD predictions where these correction factors have been applied are shown in Fig. 2. The inclusion of multi-parton interactions increase the predictions at low $E_T^{\rm jet}$ and large $\eta^{\rm jet}$. The best description of the data is observed for $p_{T,\rm min}^{\rm sec} = 1.5$ GeV.

4. Comparison of different jet algorithms

Differential cross sections for inclusive-jet photoproduction as functions of $E_T^{\rm jet}$ and $\eta^{\rm jet}$ were measured for the k_T, anti-k_T and SIScone jet algorithms. The hadronisation corrections are largest for the SIScone algorithm while similar corrections were found for the k_T and anti-k_T algorithms. As shown for the k_T algorithm above, the measurements based on anti-k_T and SIScone are well described by NLO QCD except at large $\eta^{\rm jet}$.

To compare the different jet algorithms in detail, the rations of the measured cross sections anti-k_T/k_T, SIScone/k_T and anti-k_T/SIScone were determined and are shown in Fig. 3. The cross

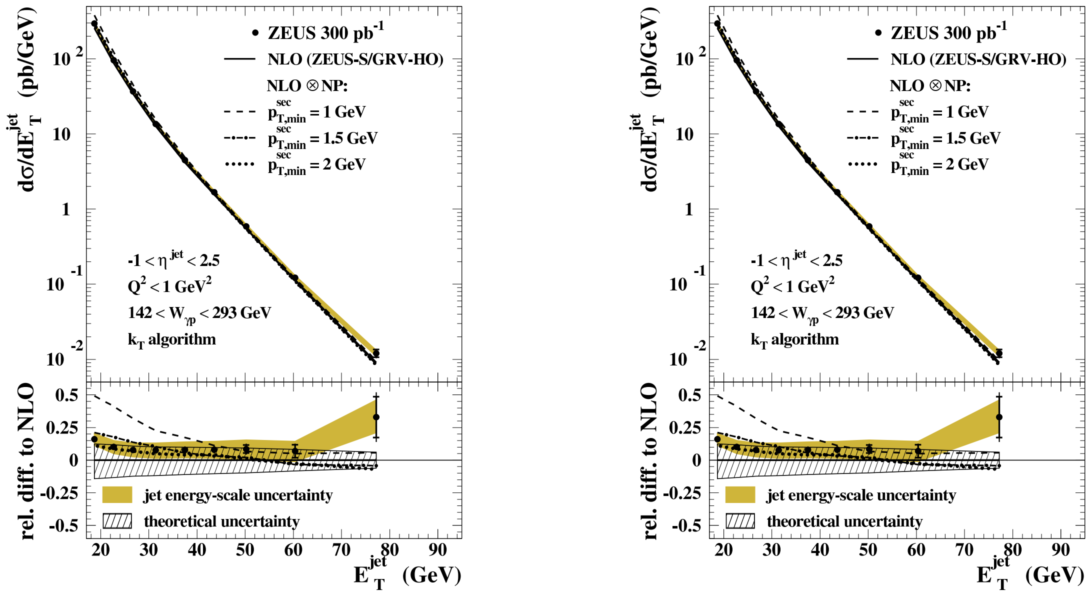

Figure 2: Single-differential cross sections $d\sigma/dE_T^{\rm jet}$ (left) and $d\sigma/d\eta^{\rm jet}$ (right) based on the k_T algorithm. The data are compared to NLO QCD predictions. For comparison, the NLO QCD calculations including an estimation of non-perturbative effects are shown in addition.

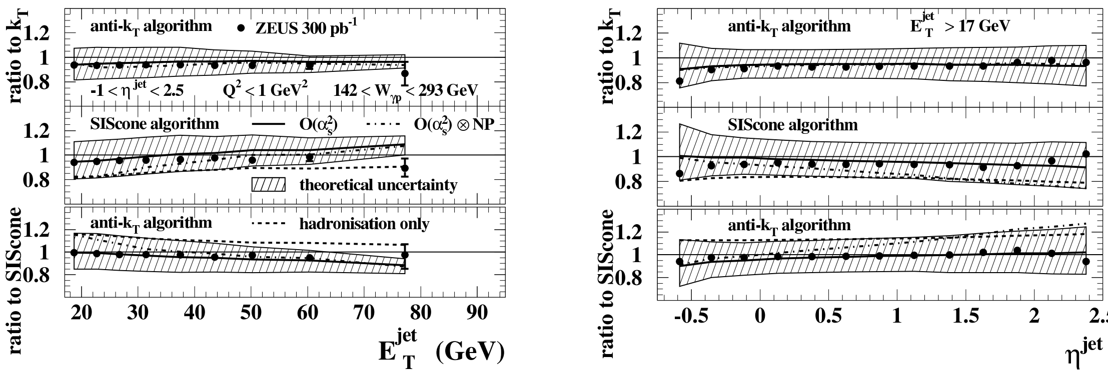

Figure 3: The ratios of the measured cross sections anti-k_T/k_T, SIScone/k_T and anti-k_T/SIScone as functions of $E_T^{\rm jet}$ (left) and $\eta^{\rm jet}$ (right).

sections for anti-k_T have the same shape as those for k_T, but are about 6% smaller. The measured cross sections based on SIScone have a slightly different shape than those based on k_T or anti-k_T. The QCD calculations with up to three partons in the final state describe the measured ratios.

5. Determination of α_s and its energy-scale dependence

The measured single-differential cross sections $d\sigma/dE_T^{\rm jet}$ for $21 < E_T^{\rm jet} < 71$ GeV based on the k_T, anti-k_T and SIScone jet algorithms were used to determine $\alpha_s(M_Z)$ [14]. Consistent results were obtained for all three jet algorithms:

$$\alpha_s(M_Z)|_{k_T} = 0.1206\ ^{+0.0023}_{-0.0022}\ (\text{exp.})\ ^{+0.0042}_{-0.0035}\ (\text{th.}),$$
$$\alpha_s(M_Z)|_{\text{anti}-k_T} = 0.1198\ ^{+0.0023}_{-0.0022}\ (\text{exp.})\ ^{+0.0041}_{-0.0034}\ (\text{th.}),$$
$$\alpha_s(M_Z)|_{\text{SIScone}} = 0.1196\ ^{+0.0022}_{-0.0021}\ (\text{exp.})\ ^{+0.0046}_{-0.0043}\ (\text{th.}).$$

The results are in agreement with other determinations of $\alpha_s(M_Z)$ [11]. In addition, values of α_s were extracted at the mean values, $\langle E_T^{\text{jet}} \rangle$, of the bins in E_T^{jet} without assuming the running of α_s. The extracted values of α_s as a function of E_T^{jet} are shown in Fig. 4. This measurement confirms the running of α_s over a wide E_T^{jet} range. The observed running is in good agreement with the two-loop QCD prediction.

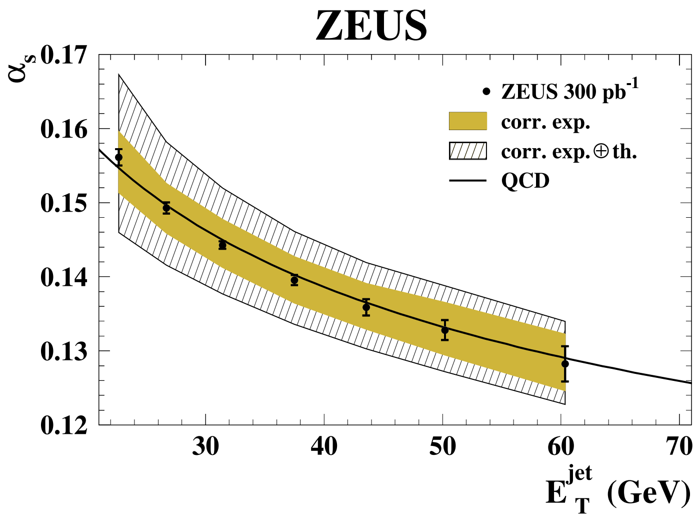

Figure 4: α_s extracted at various $\langle E_T^{\text{jet}} \rangle$ values from the measured $d\sigma/dE_T^{\text{jet}}$ cross sections based on the k_T algorithm.

6. Summary and conclusions

Inclusive-jet cross sections in photoproduction were measured using the ZEUS detector. The data are generally well described by NLO QCD predictions. The inclusion of multi-parton interactions improves the predictions at low E_T^{jet} and large η^{jet}. The presented measurements have the potential to improve the photon and proton PDFs in future QCD fits. The strong coupling constant was extracted at the Z mass with competitive precision compared to other measurements and over a wide E_T^{jet} range.

References

[1] S. Catani et al., *Longitudinally-invariant $k_\perp$-clustering algorithms for hadron-hadron collisions*, Nucl. Phys. **B 406**, 187 (1993).

[2] S.D. Ellis and D.E. Soper, *Successive combination jet algorithm for hadron collisions*, Phys. Rev. **D 48**, 3160 (1993).

[3] M. Cacciari, G.P. Salam and G. Soyez, *The anti-k_t jet clustering algorithm*, JHEP **04**, 063 (2008).

[4] G.P. Salam and G. Soyez, *A practical seedless infrared-safe cone jet algorithm*, JHEP **05**, 086 (2007).

[5] M. Klasen, T. Kleinwort and G. Kramer, *Inclusive jet production in γp and $\gamma\gamma$ processes: direct and resolved photon cross sections in next-to-leading order QCD*, Eur. Phys. J. **C 1**, 1 (1998).

[6] S. Chekanov et al., *ZEUS next-to-leading-order QCD analysis of data on deep inelastic scattering*, Phys. Rev. **D 67**, 012007 (2003).

[7] M. Glück, E. Reya, A. Vogt, *Parton structure of the photon beyond the leading order*, Phys. Rev. **D 45**, 3986 (1992);
M. Glück, E. Reya, A. Vogt, *Photonic parton distributions*, Phys. Rev. **D 46**, 1973 (1992).

[8] T. Sjöstrand, *High-energy-physics event generation with PYTHIA 5.7 and JETSET 7.4*, Comput. Phys. Comm. **82**, 74 (1994).

[9] G. Marchesini et al., *HERWIG 5.1 - a Monte Carlo event generator for simulating hadron emission reactions with interfering gluons*, Comput. Phys. Comm. **67**, 465 (1992);
G. Corcella et al., *HERWIG 6: an event generator for hadron emission reactions with interfering gluons (including supersymmetric processes)*, JHEP **01**, 010 (2001).

[10] T. Sjöstrand and M. van Zijl, *A multiple-interaction model for the event structure in hadron collisions*, Phys. Rev. **D 36**, 2019 (1987).

[11] H. Abramowicz et al., *Inclusive-jet photoproduction at HERA and determination of α_s*, Nucl. Phys. **B 864**, 1 (2012) [`arXiv:1205.6153`].

[12] F.D. Aaron, *Combined measurement and QCD analysis of the inclusive $e^{\pm}$ scattering cross sections at HERA*, JHEP **01**, 109 (2010).

[13] A.D. Martin et al., *Parton distributions for the LHC*, Eur. Phys. J. **C 63**, 189 (2009).

[14] S. Chekanov et al., *Inclusive jet cross sections in the Breit frame in neutral current deep inelastic scattering at HERA and determination of α_s*, Phys. Lett. **B 547**, 164 (2002).